

# Short-Term Scheduling of Cryogenic Energy Storage Systems in Microgrids Considering CHP-Thermal-Heat-Only Units and Plug-in Electric Vehicles

S. Cheshme-Khavar<sup>1</sup>, A. Abdolahi<sup>2,\*</sup>, F.S. Gazijahani<sup>2</sup>, N.T. Kalantari<sup>2</sup>, J.M. Guerrero<sup>3</sup>

<sup>1</sup> Department of Electrical Engineering, Amirkabir University of Technology, Tehran, Iran

<sup>2</sup> Department of Electrical Engineering, Azarbaijan Shahid Madani University, Tabriz, Iran

<sup>3</sup> Center for Research on Microgrids (CROM), AAU Energy, Aalborg University, 9220 Aalborg, Denmark

**Abstract**— With the exponential penetration of renewable energy sources (RES), the need for compatible scheduling of these has increased from economic and environmental points of view. Due to the high-efficiency and fast-response features of combined heat and power (CHP) generation units, these units can immunize the system against RES fluctuations. To address the operational challenges associated with RES, this paper aims to schedule the arbitrage of cryogenic energy storage (CES) not only to maximize its owner but also to minimize RES variability. On the other hand, plug-in electric vehicles (PEV) are applied in the proposed model as responsible loads to smooth the system's load profile by changing the consumers' consumption patterns. The proposed problem is modeled as second-order cone programming and solved by the dominated group search optimization algorithm. To verify the applicability and effectiveness of the proposed approach, four different case studies have been executed.

**Keywords**— Cryogenic energy storage, Energy arbitrage, Microgrid, Plug-in electric vehicles, Renewable energy sources.

## NOMENCLATURE

### Acronyms

ASU	Air separation unit
CES	Cryogenic energy storage
CHP	Combined heat and power
CRS	Convex region surrogate
DGSO	Dominated group search optimization
DRP	Demand response program
ESS	Energy storage systems
MG	Microgrids
PDF	Probability distribution function
PEV	Plug-in electric vehicles
RES	Renewable energy sources
SOCP	Second-order cone programming
TOC	Total organic carbon

### Parameters

$\alpha_i, \beta_i, \lambda_i$	Fuel cost coefficients of thermal units
$\alpha_j, \beta_j, \lambda_j, \delta_j, \theta_j, \varepsilon_j$	Fuel cost coefficients of CHP units
$\alpha_m, \beta_m, \theta_m$	Fuel cost coefficients of the heat-only power unit
$\rho_{ei}, \sigma_{ei}, \tau_{ei}$	Emission coefficients of conventional units
$\rho_{ej}, \sigma_{ej}, \tau_{ej}$	Emission coefficients of CHP units
$\rho_{em}, \sigma_{em}, \tau_{em}$	Emission coefficients of a heat-only unit
$a^{lin}, b^{lin}$	Coefficient demand vs. price
$D_{max}$	The maximum number of switching between charge & discharge state over

$EX_{max}^{EV-C}$

$P_{max}^{EV-D}$

$P_{min,max}^{CHP}$

$P_{min,max}^{Grid}$

$P_{min,max}^h$

$P_{min,max}^{th}$

$SoC_{max}^{EV}$

$SoC_{min}^{EV}$

$TP_{-max}$

$UR, DR$

$UT, DT$

**Sets and indices**

$i$

$j$

$k$

$m$

$N_{CES}$

$N_{CHP}$

$N_h$

$N_{th}$

$N_t$

$t$

**Variables**

$\Delta D_t$

$Pr_t$

$B_{k,t}^{CES}$

the parked time

Maximum curtailable daily load

Maximum amount of power charged by the EV

Maximum amount of power discharged by the EV

Upper and lower production limits of CHP units

Maximum and minimum power transactions with upstream grid

Upper and lower production limits of heat only power units

Upper and lower production limits of thermal units

Maximum state of charge of EV

Minimum state of charge of EV

Maximum duration of EV attendance in the parking lot

Pickup/drop off rate of load

Minimum up/down time of load

Index for thermal units

Index for CHP units

Index for CES systems

Index for heat only units

Set of CES systems

Set of CHP units

Set of heat only units

Set of thermal units

Set of time

Index for time

Amount of curtailed load at time  $t$

Virtual generation marginal cost at time  $t$

Operational cost coefficient of  $k$ th CES

Received: 10 Jun. 2022

Revised: 11 Jan. 2023

Accepted: 26 Mar. 2023

\*Corresponding author:

E-mail: a.abdollahi@azaruniv.ac.ir (A. Abdolahi)

DOI: 10.22098/joape.2023.10963.1812

**Research Paper**

© 2023 University of Mohaghegh Ardabili. All rights reserved

$B_t^{Grid}$	system at time $t$
$C_{i,t}^{th}$	Operational cost coefficient of the upstream grid at time $t$
$C_{j,t}^{CHP}$	Fuel cost of $i$ th thermal unit at time $t$
$C_{k,t}^{CES}$	Fuel cost of $j$ th CHP unit at time $t$
$C_{m,t}^h$	Operational cost of $k$ th CES system at time $t$
$C_t^{DR}$	Fuel cost of $m$ th heat-only power unit at time $t$
$C_t^{Grid}$	Operational cost of DRPs at time $t$
$D$	Fuel cost of power transaction with the upstream grid at time $t$
$D_t$	The number of switching between charge and discharge state over the parked time
$D_t^0$	Responsive load at time $t$
$E_t^{Grid}$	Initial power demand at time $t$
$e_t^{Grid}$	Emission of the upstream grid at time $t$
$EMC_{chp}$	Grid emission coefficient at time $t$
$EMC_h$	Emission cost of CHP units (\$)
$EMC_{th}$	Emission cost of heat-only unit (\$)
$EMP$	Emission cost of the thermal units (\$)
$EMS(H(m,t))$	Emission price (\$/TOC)
$EMS(P(i,t))$	Emission of $m$ th heat-only power unit at power $P$ and time $t$
$EMS(P(j,t))$	Emission of $i$ th thermal unit at power $P$ and time $t$
$H_{j,t}^{CHP}$	Emission of $j$ th CHP unit at power $P$ and time $t$
$H_{m,t}^h$	Emission of $m$ th heat-only power unit at time $t$
$H_t^D$	Heat generation of $j$ th CHP unit at time $t$
$P_1$	Heat generation of $m$ th heat-only power unit at time $t$
$P_2$	The required heat demand at time $t$
$P_{i,t}^{th}$	Cost of microgrids objective function
$P_{j,t}^{CHP}$	Pollution objective function
$P_{k,t}^{ch}$	Production of $i$ th thermal unit at time $t$
$P_{k,t}^{DIS}$	Production of $j$ th CHP unit at time $t$
$P_t^{EV-C}$	Power charged value of $k$ th CES system at time $t$
$P_t^{EV-D}$	Power discharged value of $k$ th CES system at time $t$
$P_t^{Grid}$	Amount of power charged by the EV at time $t$
$SoC_t^{EV}$	Amount of power discharged by the EV at time $t$
$t_a$	Amount of power purchased/sold from the upstream grid at time $t$
$t_d$	State of charge of EV at time $t$
$T_p$	The arrival time of EV to the parking lot
$V_t$	The departure time of EV from the parking lot
$X_t^{on/off}$	Duration of EV attendance in the parking lot
	Curtailed demand state
	Off/On time of load

## 1. INTRODUCTION

Over the past decades, the electric power industry affected by considerable changes in response to the rising concerns of global climate change and volatile fossil fuel prices. For more reliable, impressive, and eco-friendly energy production, it is essential to develop renewable energy sources (RES), particularly solar energy, along with energy storage systems (ESS). This procedure has derived into the meaning of a microgrid (MG), which can be described as a cluster of RES, ESS, and local loads, managed by an intelligent energy management system [1–3]. MG is smaller, reliable distribution networks generally installed nearby the consumers and often include hybrid energy resources, storage such as batteries, fuel cells, cryogenic energy storage (CES),

and controllable loads. Conventional power systems are typically large-scale systems in which power plants produce high-voltage electricity delivered to low-voltage customers. A significant amount of electrical energy is lost during power transmission due to the vast distance between the producer and the end-users. In this context, MGs have been widely adopted throughout the world as a way of addressing RES's significant effects and lowering CO2 emissions while aiming to handle supply-demand control at a more local level [4], [5].

The author presented a multi-objective optimization and stochastic programming method in [6] to solve the proposed mixed-integer nonlinear programming in MG. By applying the proposed method, the total operation cost of MG is reduced, and the produced power by CHP and MT is reduced to lower values. A day-ahead scheduling of multi-carrier CHP-based MGs in the presence of renewable energy sources are presented in [7]. In order to handle the uncertainties of renewables, information gap decision theory is utilized. Also, demand response model are considered for both electrical and thermal loads. The gray wolf optimization algorithm is applied to solve the economic-environmental scheduling of integrated combined heat and power, heat only, and traditional thermal units considering the effects of temperature drop of the heat pipelines [8]. In [9], it was suggested a demand response program (DRP) find the optimal scheduling of combined heat and power (CHP)-based MGs. The proposed model can cover the total electrical and thermal demands concerning economic criteria. Two main categories of DRPs containing incentive-based and time-based programs have been discussed in [10] for the MGs operation. A short-term operation scheduling of MGs among interdependent electricity and natural gas networks considering the uncertainties and DRPs addressed in [11]. The participation of DRP can reduce operating costs and improve security margins in microgrids with electricity and natural gas networks.

The authors in [12] investigated a multi-party energy management formulation for CHP-MG with hybrid DRPs that include electricity and heating demand. Short-term probabilistic scheduling of thermal power generation and wind power integrated with cryogenic energy storage systems and execution of a time-based demand response program with the aim of profit maximization and cost minimization is presented in [13]. A stochastic multi-objective optimization algorithm is suggested in [14] to minimize the energy cost and air pollution for a typical residential MG in the presence of storage. This mentioned optimization problem is modeled as a mixed-integer linear programming problem that is executed in GAMS and solved by CPLEX. This work also solved for residential MG equipped with auxiliary boiler with considering thermal and battery energy storages [15]. Optimal scheduling of heating, power, and hydrogen-based microgrid incorporated with renewables and plug-in electric vehicles are investigated in [16]. The fuel-cell-based hydrogen is integrated into the multi-energy system to investigate the power-to-hydrogen and hydrogen-to-power technologies in the model. Optimal heat and power scheduling of grid connected-MG by considering environmental issues in the presence of DRPs are discussed in [17]. An intelligent energy management system was investigated in [18] for scheduling an interconnected MG including distributed energy resources, ESS, and CHP units; to supply the electrical and thermal load demands.

According to the literature review, there are many works have been done in the optimal scheduling of microgrids in the presence of renewable energy sources field to provide electric power shortage, prevent environmental emissions, and improve some system technical specifications such as voltage profile and power losses. In some references, plug-in electric vehicles and various kind of energy storage systems have been considered for the optimal scheduling of microgrids, which results in reducing the microgrids operating costs, improving voltage profile, potential shifting of charging to the off-peak period, and discharging during

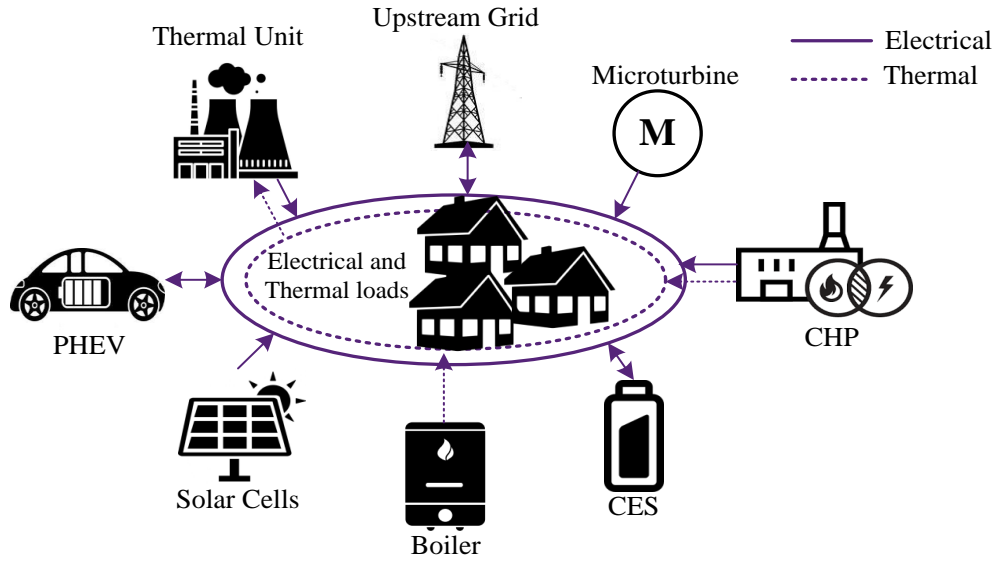


Fig. 1. Structure of proposed MG model

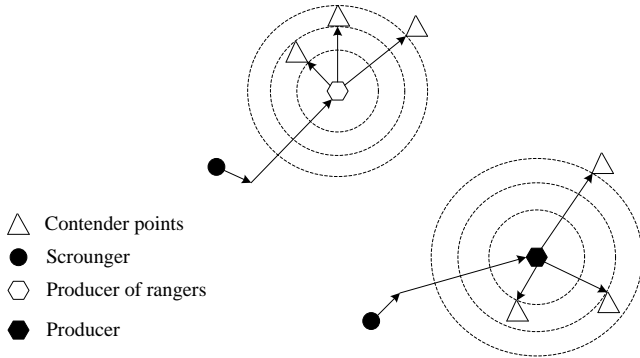


Fig. 2. Moving paths of DGSO members

the on-peak period to minimize the system loading. Due to the explanations, valuable works is done on the optimal scheduling of microgrids, but there are still many problems and deficiencies that need to be addressed properly. Briefly, the shortcomings of previous references are as follows:

- Simultaneous energy management of plug-in electric vehicles, CHP-thermal-heat-only units, and cryogenic energy storages in microgrids are not investigated.
- Energy management of plug-in electric vehicles is performed only from the owners' viewpoints, But it is not operated from the distribution system operator viewpoint.
- Effects of integration of CHP, thermal and heat only units on environmental emission and total cost reduction are not considered.

So, to address the shortcomings and drawbacks of previous literature, this paper attempts to provide the following contributions. The main novel contributions of the paper are as below:

- Utilizing the CES system as a fast-response resource to mitigate the sharp fluctuation of solar generations and maximize renewable power harvesting.
- Formulation of the problem as a computationally efficient second-order cone programming model and utilizing DGSO algorithm to minimize the MG operating cost considering various spatial-temporal constraints.
- Applying an interactive energy scheduling on the EVs, CHP units, and CES not only to reach the minimum operating cost, but also increase the profits of MG owners.

- Optimal arbitrage of EVs as a price-responsive loads in order to reduce the CO<sub>2</sub> emission and renewable swings in balancing market.
- Developing an integrated CHP-thermal-heat-only system for satisfying demands for heat and power, providing a spinning reserve for power, and reducing CO<sub>2</sub> emission.

The rest of this paper is organized as follows. Section 2 shows the modeling of CES and solar cells; Section 3 presents problem formulation and constraints of the proposed method; Section 4 describes an overview of the DGSO algorithm; simulation and numerical results are discussed in section 5; and finally, in Section 6, concluding remarks are drawn.

## 2. MODELING OF CES AND SOLAR CELLS

The structure of MG in the presence of integrated CHP-thermal-heat-only units considering PEV and solar cells is presented in Fig. 1.

### 2.1. Modeling of solar cells

The two main factors that influence the output power of solar panels, creating variations and potential behavior, are angle and solar irradiation. These parameters' probability distribution function (PDF) can be created using a variety of PDFs [19]. Two parameters,  $y$  and  $q$ , have used the Log-Normal PDF to predict the output power produced by solar irradiation according to Eq (1).

$$PDF(x) = \frac{1}{qx\sqrt{2\pi}} \exp\left[-\frac{1}{2}\left(\frac{\ln(x) - y}{q}\right)^2\right], \quad x \geq 0 \quad (1)$$

Finally, Eq. (2) yields the quantity of electricity produced by solar cells, which is dependent on the ambient temperature and sun irradiation. The temperature of the cells was determined using Eq. (3).

$$P_t^{PV} = P_{STG} + \frac{G_{ING}}{G_{STG}} \times (1 + K(T_c - T_{c,ref})) \quad (2)$$

$$T_c = T_a + \frac{N_{OT} - 20}{0.8} \times G \quad (3)$$

## 2.2. Modeling of CES

The CES plays an important function in MGs since it is intended to moderate peak demand and store excess energy in the condition of liquid air. Two Liquefaction and Expansion stages are incorporated in the construction of CES [20]. Each segment has a separate method that is discussed in the next section.

### A) Liquefaction process

Already, the procedure of air liquefaction was monopolized by the Linde Company and generated liquid from gases. At first, atmospheric air is pressurized at 60-90 pounds per square inch (PSIG). In the following, the pressurized air is refined from the humidity, carbon dioxide, and hydrocarbons. Cold boxes are used to freeze the purified compressed air in the next step. Distillation pillars and heat converters are examples of cold boxes. The liquefaction process produces three materials in general: liquid argon (LAr), liquid nitrogen (LN2), and liquid oxygen (LO2) [21].

### B) Expansion process

The liquefied air is pushed first to pressurize the cryogenic liquid air. The ambient heat from the frozen compressed liquid air is absorbed via heat converters. After that, the turbine and generator create high-pressure gaseous air. Because of the energy loss, the round-trip efficiency is roughly 40%. On the other hand, using industrial waste heat as auxiliary heat may achieve a round trip efficiency of up to 70%. Liquid gas is forced to create high-pressure liquid. A low-grade heat source is subsequently used to evaporate the created liquid. To produce power, a high-pressure cold gas turbine will be employed [22]. The advantages of using CES as a new technology and for energy storage are discussed in this section. The modeling of an air separation unit (ASU) is quite intricate, and the method is extremely difficult. As a consequence, the ASU technique is separated into several styles with convex regions in which the ASU has a linear connection between power consumption and ASU production. The three modes of the ASU system are "off," "start-up," and "production." To mimic the various forms of ASU, the Convex Region Surrogate (CRS) model is employed. A collection of convex sub-regions is employed to produce the potential region in the CRS model [23]. The ASU model is represented in the following fashion, according to the CRS:

$$P_t^{ASU} = \sum_m \sum_{q \in R_m} \left( \delta_{mq} \bar{y}_{mqt} + \sum_i \gamma_{mqr} \bar{P}A_{mqrt} \right) \quad (4)$$

$$PA_t^r = \sum_m \sum_{q \in R_m} \bar{P}A_{mqrt}, \quad r \in \{LN_2, LO_2, LAr\} \quad (5)$$

$$\bar{P}A_{mqrt} = \sum_{j \in J_{mq}} \lambda_{mqjt} v_{mqjr} \quad (6)$$

$$\sum_{j \in J_{mq}} \lambda_{mqjt} = \bar{y}_{mqt} \quad (7)$$

$$y_{mt} = \sum_{q \in R_m} \bar{y}_{mqt} \quad (8)$$

$$\sum_m y_{mt} = 1 \quad (9)$$

Based on liquid production, Eq. (4) predicts the value of ASU-consumed power. Eqs. (5) to (9) also indicate the limits of ASU modeling.

## 3. PROBLEM FORMULATION

### 3.1. Objective function

In this paper, the objective function (10) is presented as a single-objective form to minimize the microgrid operating cost and the environment emission cost, where the first term (P1) includes the costs of thermal units, cryogenic energy storage operation, PV power generation, power trade-off with the upstream grid, and plug-in electric vehicle arbitrage. The second term (P2) includes the cost of environmental emission generated by thermal, CHP, and heat-only units. In order to sum these to terms, the second term (P2) is multiplied by the penalty cost and converted to the cost function.

$$\min F = (P_1 + P_2) \quad (10)$$

### 3.2. Operating cost function of MG

The purpose of Eq. (11) is to minimize the total operating cost of MG, including CES systems, responsive loads, and various kinds of thermal power systems like conventional systems, cogeneration systems, and heat-only systems. All of the functions mentioned earlier cumulated in Eq. (11).

$$P_1 = \sum_{t=1}^{24} \left\{ \sum_{i=1}^{N_{th}} C_{i,t}^{th} + \sum_{j=1}^{N_{CHP}} C_{j,t}^{CHP} + \sum_{m=1}^{N_h} C_{m,t}^h + \sum_{k=1}^{N_{CES}} C_{k,t}^{CES} + C_t^{PV} + C_t^{Grid} \right\} \quad (11)$$

where,  $C^{th}$ ,  $C^{CHP}$ ,  $C^h$ ,  $C^{CES}$ , and  $C^{Grid}$  demonstrates the cost function of thermal units, CHP units, heat-only systems, CES, and power transaction with the upstream grid, respectively. The traditional thermal unit total nonlinear cost modeled as Eq. (12):

$$C_{i,t}^{th} = \alpha_i + \beta_i (P_{i,t}^{th}) + \lambda_i (P_{i,t}^{th})^2 \quad (12)$$

The CHP system total cost presented as Eq. (13):

$$C_{j,t}^{CHP} = \alpha_j + \beta_j P_{j,t}^{CHP} + \lambda_j (P_{j,t}^{CHP})^2 + \delta_j H_{j,t}^{CHP} + \theta_j (H_{j,t}^{CHP})^2 + \xi_j H_{j,t}^{CHP} P_{j,t}^{CHP} \quad (13)$$

The heat-only system cost function can be formulated as Eq. (14):

$$C_{m,t}^h = \alpha_m + \partial_m H_{m,t}^h + \theta_m (H_{m,t}^h)^2 \quad (14)$$

The operation cost of solar cells presented as Eq. (15) [24]:

$$C_t^{PV} = \sum_{t=1}^{24} (P_t^{PV} \times \Psi_t) \quad (15)$$

The CES cost function described as Eq. (??):

$$C_{k,t}^{CES} = \sum_{k=1}^{N_{CES}} B_{k,t}^{CES} \times (P_{k,t}^{Dis} - P_{k,t}^{Ch}) \quad (16)$$

Finally, the network cost function [24] derived as Eq. (17):

$$C_t^{Grid} = P_t^{Grid} \times \Omega_t \quad (17)$$

where,  $P^{Grid}$  shows the amount of electric power, which is transacted with the upstream grid at time t and  $\Omega_t$  represents the utility bid at time t. Effective charging/discharging scheduling of PEVs decreases power losses and minimizes microgrid operating costs. The charging/discharging cost of PEVs is presented as (18) [25].

$$C^{PEV} = \sum_{t=1}^{24} \sum_{n=1}^{N_{PEV}} \left[ b \times P_{n,t}^{Ch/Dis} + P_{n,t}^{Ch} \times C^{Ch} - P_{n,t}^{Dis} \times C^{Dis} \right] \quad (18)$$

### 3.3. Environmental emission cost function

The second objective function focused on minimizing the amount of CO<sub>2</sub> emission generated by thermal, CHP, and heat-only units. Environmental emission-associated costs are given as follows [26].

$$P_2 = C^{Em} \quad (19)$$

$$C^{Em} = EMC_{i,t}^{th} + EMC_{j,t}^{CHP} + EMC_{m,t}^h \quad (20)$$

$$EMC_{i,t}^{th} = EMP^{th} \times \sum_{t=1}^{24} \sum_{i=1}^{N_{th}} EMS(P_{i,t}^{th}) \quad (21)$$

$$EMC_{j,t}^{CHP} = EMP^{CHP} \times \sum_{t=1}^{24} \sum_{j=1}^{N_{CHP}} EMS(P_{j,t}^{CHP}) \quad (22)$$

$$EMC_{m,t}^h = EMP^h \times \sum_{t=1}^{24} \sum_{m=1}^{N_h} EMS(H_{m,t}^h) \quad (23)$$

Eqs. (19) and (20) show the total CO<sub>2</sub> emission costs function. According to equations (21-23),  $EMC_{i,t}^{th}$ ,  $EMC_{j,t}^{CHP}$  and  $EMC_{m,t}^h$  illustrate the CO<sub>2</sub> emission costs of thermal units, CHP units, and heat-only units, respectively. The operation of an integrated CHP-thermal-heat only unit is always accompanied by the release of several environmental pollutants and, the CO<sub>2</sub> emissions by units at hour  $t$  [26].

$$EMS(P_{i,t}^{th}) = \sum_{i=1}^{N_{th}} \left( \rho_{ei} + \sigma_{ei} P_{i,t}^{th} + \tau_{ei} (P_{i,t}^{th})^2 \right) \quad (24)$$

$$EMS(P_{j,t}^{CHP}) = \sum_{j=1}^{N_{CHP}} \left( \rho_{ej} + \sigma_{ej} P_{j,t}^{CHP} + \tau_{ej} (P_{j,t}^{CHP})^2 \right) \quad (25)$$

$$EMS(H_{m,t}^h) = \sum_{m=1}^{N_h} \left( \rho_{em} + \sigma_{em} H_{m,t}^h + \tau_{em} (H_{m,t}^h)^2 \right) \quad (26)$$

Equations (24-26) indicate the amount of CO<sub>2</sub> emission released by thermal units, CHP units, and heat-only units, respectively.

### 3.4. Constraints

The suggested optimization problem is surrounded by several limitations, classified as below.

#### a) Power balance

Concerning the first aim, the following constraint assures that the total demand is met across the planning horizon by the power provided by all thermal units, CESSs, and grid-supplied sources.

$$\sum_{i=1}^{N_{th}} P_{i,t}^{th} + \sum_{j=1}^{N_{CHP}} P_{j,t}^{CHP} + \sum_{k=1}^{N_{CES}} P_{k,t}^{Dis} + \sum_{e=1}^{N_{EV}} P_t^{EV,Dis} + P_t^{Grid} + P_t^{PV} = D_t + \sum_{k=1}^{N_{CES}} P_{k,t}^{Ch} + \sum_{e=1}^{N_{EV}} P_t^{EV,Ch} \quad (27)$$

#### b) Power limits

To reach stable operation, the transacted power with upstream grid, generating power by CHP units, thermal units, and heat-only power systems must be operated in their minimum and maximum limitation.

$$P_{min}^{th} \leq P_{i,t}^{th} \leq P_{max}^{th} \quad (28)$$

$$P_{min}^{CHP} \leq P_{j,t}^{CHP} \leq P_{max}^{CHP} \quad (29)$$

$$P_{min}^{Grid} \leq P_t^{Grid} \leq P_{max}^{Grid} \quad (30)$$

#### c) Heat balance

The CHP and heat-only units accountable for providing heat supply must provide heat output, at least, to coverage heat demand.

$$H_t^D = \sum_{j=1}^{N_{CHP}} H_{j,t}^{CHP} + \sum_{m=1}^{N_h} H_{m,t}^h \quad (31)$$

#### d) Heat limits

Output heat of CHP and heat only units must be operating in their lower and upper bounds as constraints (32), (33).

$$H_{min}^{CHP} \leq H_{j,t}^{CHP} \leq H_{max}^{CHP} \quad (32)$$

$$H_{min}^h \leq H_{m,t}^h \leq H_{max}^h \quad (33)$$

#### e) Minimum up/down time

The minimum up/down time constraints related to the traditional thermal units are presented as constraints (34), (35).

$$T_{i,t}^{ON} \geq MUT_i \quad (34)$$

$$T_{i,t}^{OFF} \geq MUT_i \quad (35)$$

#### f) CES constraints

Some constraints on charge and discharge rate of CES systems are listed as follows:

$$W_t^{CES} = W_{t-1}^{CES} + \Delta t \left( \eta^{Ch} P_t^{Ch} - P_t^{Dis} / \eta^{Dis} \right) \quad (36)$$

$$W_{min}^{CES} \leq W_t^{CES} \leq W_{max}^{CES} \quad (37)$$

$$P_t^{Ch} \leq P_{max}^{Ch} \quad (38)$$

$$P_t^{Dis} \leq P_{max}^{Dis} \quad (39)$$

$$W_0^{CES} = W_{24}^{CES} \quad (40)$$

#### g) EV constraints

The vehicles park in the parking lot for specific hours, and the vehicles owner charge and discharge them during this period. Therefore, vehicles play the role of variable programmable loads. Limitation of  $P_t^{EV,Ch}$  and  $P_t^{EV,Dis}$  can be considered as:

$$P_t^{EV,Ch} \leq P_{max}^{EV,Ch} \quad (41)$$

$$P_t^{EV,Dis} \leq P_{max}^{EV,Dis} \quad (42)$$

So that,  $P_{max}^{EV,Ch}$  and  $P_{max}^{EV,Dis}$  are the maximum power of electric vehicles charging and discharging. These limits determine the maximum amount of charge and discharge that the charger can offer. The electric vehicles state of charge constraints [27]:

$$SoC_{min}^{EV} \leq SoC_t^{EV} \leq SoC_{max}^{EV} \quad (43)$$

where  $SoC_{max}^{EV}$  and  $SoC_{min}^{EV}$  are the maximum and minimum amount of the electric vehicle state of charge, respectively. This limitation allows the SoC to vary between the minimum and maximum SoCs' predefined. The parking time duration is defined as:

$$T_P \leq T_{P-max} \quad (44)$$

$$T_P = t_d - t_a \quad (45)$$

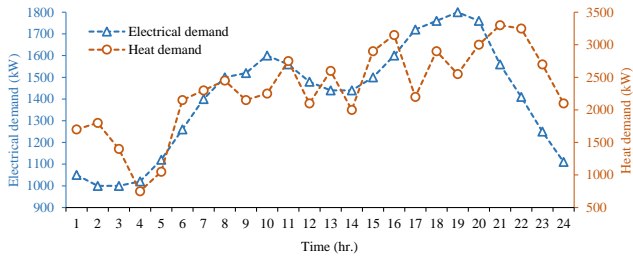


Fig. 3. Hourly both electrical and heat demand of system

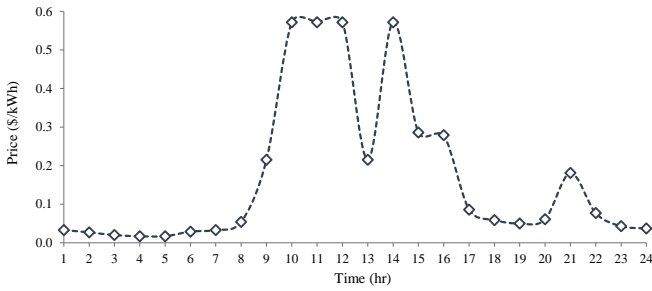


Fig. 4. Real-time market price

where  $t_a, t_d$  are the arrival and departure times of EV from parking lot.  $T_p$  is the duration of EV attendance in the parking lot. This limitation allowed the parking owners to schedule charge and discharge of each EV when they are in parking. The number of switching between charge and discharge is determined by the maximum number of switching between charge and discharge based on the time-lapse battery life of the EV.

$$D \leq D_{max} \tag{46}$$

So that  $D$  is the number of switching between charge and discharge state over the parked time and  $D_{max}$  is the maximum number of switching between charge and discharge state over the parked time.

#### 4. PROVIDING AN OVERVIEW OF DGSO ALGORITHM

The DGSO algorithm is an upgraded version of the GSO algorithm and is used to solve the suggested hard SOCP problem [28]. Therefore in portion of the study, the essential ideas of classic GSO and its improved form are explored. The GSO method is a widely used meta-heuristic optimization solution that has three different kinds of participants: producers, scavengers, and rangers. In every cycle, the creator is the participant with the greatest level of fitness. This member examines various adjacent sites in try to come up with much more suitable options. The monitoring protocol may be used by scroungers to conduct

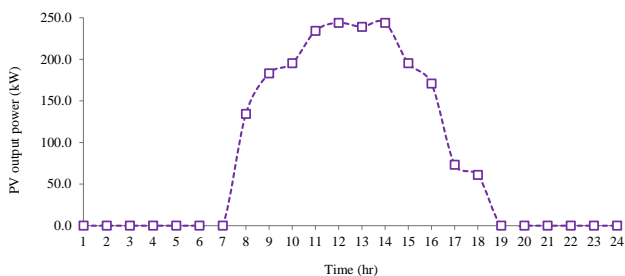
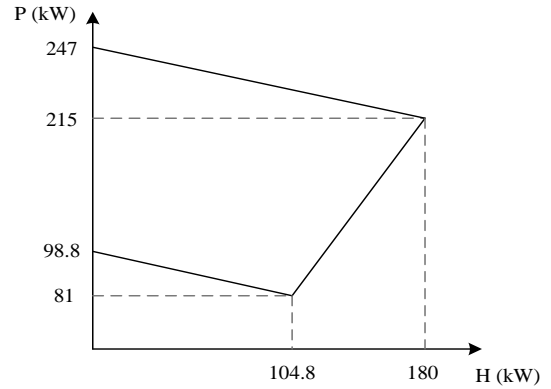
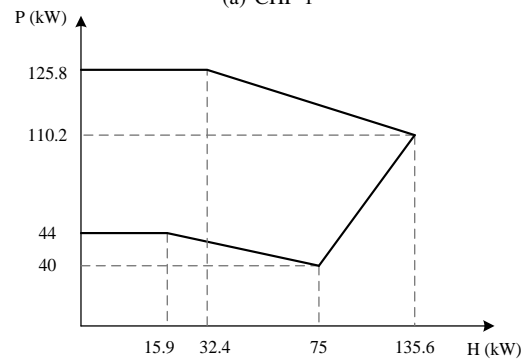


Fig. 5. PV output power curve



(a) CHP 1



(b) CHP 2

Fig. 6. Power-heat feasible region for CHP unit

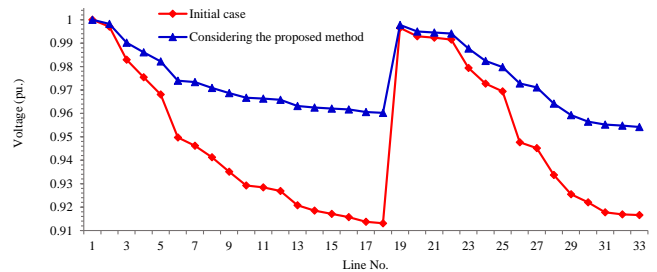


Fig. 7. Voltage magnitudes of proposed system in different cases

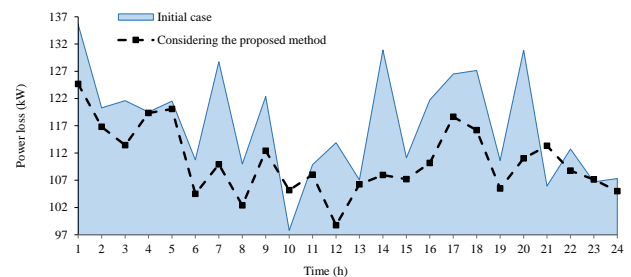


Fig. 8. Power losses of the proposed system in different cases

Table 1. The relationship between battery lifetime and number of allowable charging and discharging

Life time of CES	$AOB < 4$	$4 \leq AOB < 6$	$6 \leq AOB < 8$	$8 \leq AOB$
$N_{max}$	8	6	4	2

Table 2. Thermal, CHP and Heat-only units emission coefficients data

Unit	$\alpha_e$ (TOC)	$\beta_e$ (TOC/kWh)	$\gamma_e$ (TOC/(kWh) <sup>2</sup> )
THE1	10.33908	-0.24444	0.00312
THE2	10.33908	-0.24444	0.00312
THE3	30.03910	-0.40695	0.00509
THE4	30.03910	-0.40695	0.00509
THE5	32.00006	-0.38132	0.00344
CHP1	10.33908	-0.40659	0.00312
CHP2	10.33908	-0.40659	0.00312
HTO1	33.00056	-0.39023	0.00465

Table 3. Thermal units cost coefficients data

Unit	$P_{Min}$ (kW)	$P_{Max}$ (kW)	a (\$/(kWh) <sup>2</sup> )	b (\$/kWh)	c (\$)	MUT (hr.)	MDT (hr.)
THE1	150	700	20	0.15	0	3	3
THE2	100	450	40	0.25	0	2	2
THE3	50	300	90	0.45	0	1	1
THE4	50	1000	10	0.0133	0.002	1	1
THE5	100	1000	45	0.375	0	1	1

Table 4. CHP units cost coefficients data

Unit	$\alpha$	$\beta$	$\lambda$	$\delta$	$\theta$	$\xi$
CHP1	2650	14.5	0.0345	4.2	0.030	0.031
CHP2	1250	36.0	0.0435	0.6	0.027	0.011

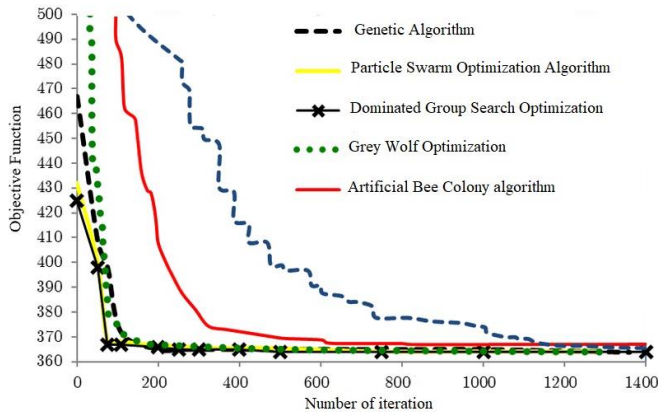


Fig. 9. Convergence curve of DGSO compared to other algorithms

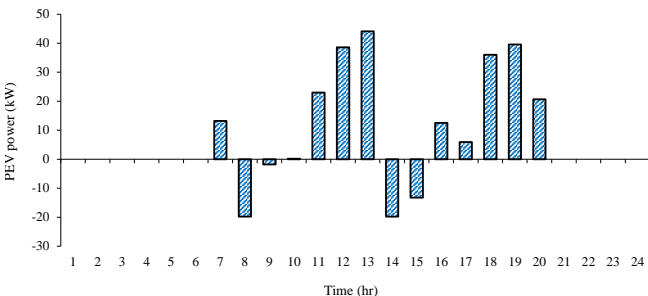


Fig. 10. Optimal energy management of PEV in the microgrid operation

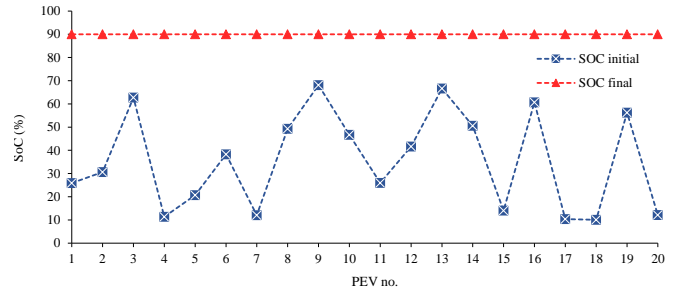


Fig. 11. The initial and final SoC of all PEVs

joining maneuvers in the orientation of the producer, making the optimization process simpler. Rangers are the third type of GSO, and they go on random hikes throughout the quest [29]. The GSO method allows any ranger to make random motions throughout the scanning space:

$$R_i^{k+1} = R_i^k + l_i D_i^k (\varphi^{k+1}), \quad l_i = a * r_1 * l_{max} \quad (47)$$

This algorithm's primary goal is to help scavengers be more productive. This program selects the scavengers who chase the producer at random. Because of this, a scavenger may follow the producer as long as the rangers are nearby. A better solution is more likely to be found in the vicinity of the producers, which might impair the correct tracking procedure. In order to determine how many present scavengers will chase the producer or the rangers' producer, the DGSO algorithm is recommended. The current scavengers are categorized depending on their proximity to the producers. Fig. 2 depicts the DGSO members' progress across the search region.

Table 5. Heat-only unit cost coefficients data

Unit	$H_{min}$ (kW)	$H_{max}$ (kW)	$\sigma$ (\$)	$\mu$ (\$/kWh)	$\rho$ (\$/(kWh) <sup>2</sup> )
HTO1	0	2695.2	950	2.0109	0.038

$$\begin{cases} X_{S,i}^{k+1} = X_{S,i}^k + r^o(|X_P^k - X_{S,i}^k|) & |X_P^k - X_{S,i}^k| < |X_{pR}^k - X_{S,i}^k| \\ X_{S,i}^{k+1} = X_{S,i}^k + r^o(|X_{pR}^k - X_{S,i}^k|) & |X_{pR}^k - X_{S,i}^k| < |X_P^k - X_{S,i}^k| \end{cases} \quad (48)$$

## 5. SIMULATION RESULTS AND DISCUSSION

### 5.1. Assumptions and require data

In this paper, a case study is considered by using the following assumptions to be considered for the arrival and departure of electric vehicles to the parking lot.

- The total number of EVs is 20.
- The maximum charging and discharging power are 6.5 kW.
- The limitation of SoC is between 10% and 90%.
- The maximum capacity of EVs is assumed 16.5 kWh.
- The arrival and departure times of EVs is randomly between 6 and 18.
- The initial charge rate of EVs when arriving to the parking lots is between 10% and 70%.
- The ESS lifetime is assumed between 2 and 9 years.
- The amount of vehicle charge at the end (when leaving the parking lot) must be full.

Moreover, the results are presented based on the following scenarios:

**Scenario I:** MG scheduling cost with and without considering CHP units

**Scenario II:** MG scheduling cost with and without considering both participating CHP and responsible loads

**Scenario III:** MG scheduling cost with and without considering the impact of CO<sub>2</sub> emission price

**Scenario IV:** Impact of real-time market price variations on MG scheduling total cost.

### 5.2. Simulation results and discussion

The exchange of power has taken place between the parking lot owner and the MG owner, so the construction cost of parking is not considered. The relationship between battery lifetime and number of allowable charging and discharging is shown as Table 1.

The electrical and heat demand of system has been depicted in Fig. 3 for 24 hours [30]. The real time market price alteration for the mentioned day is considering as Fig. 4 [31]. Fig. 5 shows the PV output power curve, which is depends on the angle and intensity of sunlight. Fig 6(a) and 6(b) shows the power-heat feasible region for CHP 1 and CHP 2, respectively, which the horizontal axis represents the heat output and the vertical axis indicates the CHP power production in kW.

Table 2 displays the thermal, CHP and Heat-only units' emission coefficient data. Table 3 gives the specifications of thermal units include fuel cost function coefficients, the minimum and maximum production capacity of units, minimum up and down time [32]. The cost coefficient data related to thermal, CHP, and heat-only units are depicted in Table 3– 5, respectively [33], [34]. The data related to CES systems includes initial and minimum/maximum state of charge, maximum power production, and charging/discharging efficiency has been given in Table 6 [35].

To supply electrical energy, solar panels, CESs, and thermal units, as well as heat generation units for the provision of thermal energy, are presumptively included in the MG. Notably, the outcomes are predicated on a solar power situation with 0% error. The simultaneous scheduling of solar panels, CES, and the power trade-off with the upstream grid, CHP, and thermal units in the

MG is shown in Table 7. To ensure that the total generation power and total MG consumption demand are equal over the course of 24 hours, this scheduling strategy is taken into account. As can be seen, the power balance constraint is fully observed in this MG scheduling. In addition, the scheduling of the units mentioned depends on the cost of the electricity purchased from the upstream grid, the best CES arbitrage, the best solar panel production, and both CHP and thermal units. In this section, unit commitment of GENCOs has been implemented to the high price generation units considered as spinning reserve by independent system operator. Table 8 illustrates the scheduling of heat-only and CHP units, which the total generation heat by the CHP and heat-only units is equal to the total heat demand of MG per hour.

The voltage profile is shown in Fig. 7 with and without taking the suggested method into account. As can be observed, the voltage profile in the initial case is not within the authorized range, but with the application of cryogenic energy storage, CHP-thermal-heat-only units, it is constrained within the permissible range. The allowable range for voltage magnitudes in all buses is set to be between 0.95 and 1.05 p.u. Implementing the suggested technique had a considerable effect on the voltage profile improvement as a result. The system power losses are displayed in Fig. 8. As can be observed, the power loss of lines in the presence of CES, CHP-thermal-heat-only units is significantly decreased.

The convergence curve related to the proposed method obtained from different algorithms is shown in Fig. 9. According to this figure, the convergence rate and speed obtained from the DGSO algorithm are higher compared to other metaheuristic algorithms such as PSO, GA, GWO, and ABC algorithms. Also, the minimum cost of MG scheduling was obtained at iteration 175.

To show the performance and privileges of the proposed model in comparison with previous works, different analysis have been executed. In order to apply your valuable suggestion, a comparative study is performed based on Table 9.

**Scenario I: MG scheduling total cost with and without considering CHP units**

The results of first case demonstrates in Table 10, which indicates that the total cost of MG scheduling after adding the CHP units has improved by 2.01 percent. This is because the CHP units with lower cost will shut down low-efficiency thermal units.

**Scenario II: MG scheduling cost with and without considering both participating CHP and responsible loads**

In this case, in addition to the thermal units, CHP, CES, and PV; EVs parking has been utilized as responsible loads. EV owners gain profit by paying less cost to the parking owners and MG gained profit from receiving the EVs charging cost and planning of their charging/discharging.

#### a) Without considering the main grid

In this case, it is assumed that the MG does not have access to the upstream grid and provides its demand independently. The total scheduling cost of MG is compared in two cases in Table 11. It is seen from the figure that the total scheduling cost reduces by 0.16% by adding responsible loads to the system compared with the initial case (without responsible loads). By utilizing both responsible loads and CHP units, the cost of generation increased (because of an increase in consumption demand), but the total cost was reduced due to the revenue from the sale of electric power to the EVs. Fig. 10 shows the optimal power of PEV parking. The goal is that, at first, the PEVs are fully charged, and then the operating cost is minimized. As can be seen, the PEVs are charged during high-cost hours and discharged during low-cost periods. Due to the randomness of the arrival and departure hours of the

Table 6. Data of CES

Unit	SoC <sub>0</sub> (kWh)	SoC <sub>min</sub> (kWh)	SoC <sub>max</sub> (kWh)	$P_{CES \max}$ (kW)
CES	1500	500	2500	500

Table 7. Scheduling of different units and upstream grid in terms of electrical

Hour	Electrical demand	Generation power									
		Thermal units					CHP		Upstream grid	PV	CES
		1	2	3	4	5	1	2			
1	1050	0	135	0	0	0	215	110	331	0	259
2	1000	0	0	73	0	158	215	110	414	0	30
3	1000	0	0	85	0	73	215	110	374	0	143
4	1020	0	0	88	103	134	215	110	280	0	90
5	1120	0	0	103	77	136	215	110	369	0	110
6	1260	0	0	114	60	113	215	110	648	0	0
7	1400	0	0	0	81	132	215	110	862	0	0
8	1500	0	0	0	133	0	215	110	1002	40	0
9	1520	0	0	0	0	0	215	110	1152	140	0
10	1600	0	0	0	0	0	215	110	1398	160	0
11	1560	150	157	0	0	0	215	110	998	200	0
12	1480	150	135	0	0	0	215	110	850	320	0
13	1440	150	168	0	0	0	215	110	571	240	0
14	1440	182	135	0	90	105	215	110	506	320	0
15	1500	173	137	0	66	90	215	110	522	200	0
16	1600	203	135	0	60	115	215	110	622	140	0
17	1720	150	135	94	97	79	215	110	690	60	90
18	1760	150	151	87	100	73	215	110	718	20	136
19	1800	0	0	126	0	99	215	110	1218	0	32
20	1700	0	0	126	0	0	215	110	1238	0	11
21	1560	0	0	86	0	0	215	110	1405	0	0
22	1410	0	0	0	0	0	215	110	1045	0	40
23	1250	0	0	0	0	0	215	110	780	0	145
24	1110	0	0	0	0	0	215	110	685	0	100

Table 8. Scheduling of CHP and heat-only units in terms of thermal

Hour	Heat demand	Generation heat		
		CHP		Heat-only
		1	2	
1	401	180	135.6	85.4
2	407	180	135.6	91.4
3	417	180	135.6	101.4
4	431	180	135.6	115.4
5	438	180	135.6	122.4
6	450	180	135.6	134.4
7	455	180	135.6	139.4
8	462	180	135.6	146.4
9	472	180	135.6	156.4
10	474	180	135.6	158.4
11	478	180	135.6	162.4
12	483	180	135.6	167.4
13	474	180	135.6	158.4
14	470	180	135.6	154.4
15	462	180	135.6	146.4
16	443	180	135.6	127.4
17	438	180	135.6	122.4
18	450	180	135.6	134.4
19	462	180	135.6	146.4
20	474	180	135.6	158.4
21	468	180	135.6	152.4
22	449	180	135.6	133.4
23	430	180	135.6	114.4
24	414	180	135.6	98.4

Table 9. Comparison study on different methods in the proposed field

Ref.	Proposed method	Total operating cost reduction (%)
[36]	Optimal energy management of smart renewable-based microgrid considering PEV	6.71
[37]	Optimal scheduling of microgrid with storage considering load and renewable uncertainty	6.96
[38]	Stochastic optimal scheduling of CHP-FC, WT, PV and hydrogen storage in microgrids	5.24
[39]	Day-ahead economic scheduling of microgrids equipped with PEVs	6.77
[40]	Stochastic optimal scheduling of demand response-enabled microgrids with renewables	6.10
[41]	Optimal scheduling of combined cooling, heating, and power microgrid	2.27
[42]	Optimal scheduling of reconfigurable microgrids incorporating the PEVs and uncertainties	5.70
[43]	Optimal scheduling of renewable-based microgrid with photovoltaic system and storage	2.24
This paper	Short-Term Scheduling of Cryogenic Energy Storage Systems in Microgrids Considering CHP-Thermal-Heat-Only Units and Plug-in Electric Vehicles	7.17

Table 10. MG scheduling total cost with and without considering CHP units

Case	Cost (\$)	Improvement (%)
With CHP units	53.709	-
Without CHP units	52.631	2.01

Table 11. MG scheduling cost with and without considering both participating CHP and responsible loads

Case	Parking income (\$)	Generation cost (\$)	Total cost (\$)	Improvement (%)
With responsible loads	0	52.631	52.631	-
Without responsible loads	153	52.700	52.547	0.16

Table 12. MG scheduling cost with and without considering the impact of CO<sub>2</sub> emission price

Case	Total cost (\$)	Pollution (kg)	Improvement (%)
Without CO <sub>2</sub> emission price	52.547	1421	-
With CO <sub>2</sub> emission price	52.580	1350	5.00

PEVs and the limitation of these hours, charging may also take place at low prices. The initial and final SoC of all PEVs is shown in Fig. 11. According to this graph, the final SoC of all PEVs is fully charged, and their initial SoC is changing between 10 and 70%.

#### b) With considering the main grid

In this case, due to the lower price of the upstream network than CHP and thermal units, the use of electric car parking is not profitable.

#### Scenario III: MG scheduling cost with and without considering the impact of CO<sub>2</sub> emission price

The penalty factor of CO<sub>2</sub> emission has been considered for MG scheduling total cost, which the penalty factor of CO<sub>2</sub> emission is assumed 0.0266 \$/kg. If the cost of pollution is taken into account, the total cost will be increased, but the amount of produced pollution will be reduced by 71 kg compared to regardless of the pollution cost. Every 5 kg of pollution that is reduced, the MG scheduling total cost will increase to the amount of 33 \$. This increase in MG scheduling total costs to reduce this level of pollution is negligible and can be compensated.

#### Scenario IV: Impact of real-time market price variations on MG scheduling cost

In this case, the real-time market price investigates. Table 12 compares the results in four modes (present electricity price, \*electricity price, 2\*electricity price, and 4\*electricity price). With a drop in electricity prices, the proportion of electricity sales to EVs parking is significantly lower than the charging cost of EVs, and the use of DRP will not be cost-effective. With increasing the electricity price, revenue from power sales to EVs increases, and the total cost of the system is reduced. However, electricity purchases from the upstream grid are not profitable and thermal units must provide all system requirements demand, therefore, the

total cost of the system increases. By quadrupling the electricity price, the revenue from power sales to EVs obtained more than the power production cost, so the total cost will be reduced.

## 6. CONCLUSION

In this paper, an energy storage system was used to provide an arbitrage opportunity for the system operator to reduce its operational expenditures. In this model, various instruments such as CHP-thermal-heat-only units and EV fleets are employed to aid the system operator to achieve the targets in an economic-environmental manner. The EVs are modeled as responsible loads to smooth the load profile of the system and hedge the operator against the risk of unforeseen conditions. The features of the proposed model are non-linear, non-convex, and non-smooth. This is why we use the DGSO algorithm to solve this complicated SOCP problem. The DGSO finds the best optimal solutions at the minimum operating cost of the system. The best solution includes optimal arbitrage of CESs and EVs as well as optimal production of RES. By applying the proposed approach, the operating cost of MGs has considerably reduced while minimum air pollution is released. Based on the results, the following findings are achieved:

- The use of CHP-thermal-heat only unit reduces the operational cost of MGs. This issue will be associated with a slight increase in air pollution.
- Despite increasing production costs by using CES, it reduces the total cost of MG. The storage device by applying energy arbitrage between low-load and high-load hours reduces the distance between low-load and high-load demand, and as a result, reduces the cost of supplying consumers by reducing locational marginal prices.
- The amount of air pollution alleviates by penalty factor of CO<sub>2</sub> emission, and the network operator, by determining the

Table 13. Impact of real-time market price variations on MG scheduling total cost

Case	Parking income (\$)	Generation cost (\$)	Total cost (\$)
Present electricity price	153	52.700	52.547
* electricity price	0	52.631	52.631
2 * electricity price	306	52.900	52.594
4 * electricity price	612	52.900	52.288

amount of the penalty coefficient according to his risk seeker or risk aversion strategies, achieves a fair state between economic costs and air pollution.

- The EVs operation that can act as a demand flexibility option is strongly depends on the price of electricity and operation conditions of the system.

### REFERENCES

- [1] N. Hatzigiorgiou, "Architectures and control," Microgrids: John Wiley & Sons, 2014.
- [2] H. Liang, W. Zhuang, "Stochastic modeling and optimization in a microgrid: A survey," *Energies*, vol. 7, no. 4, pp. 2027–2050, 2014.
- [3] T. A. Nguyen, M. L. Crow, "Stochastic optimization of renewable-based microgrid operation incorporating battery operating cost," *IEEE Trans. Power Syst.*, vol. 31, no. 3, pp. 2289–2296, 2016.
- [4] P. Piagi, R. H. Lasseter, "Autonomous control of microgrids," in proc. of the *Power Eng. Society General Meeting*, Montreal, QC, Canada, 2006, pp. 8–pp.
- [5] Y. Zheng, B.M. Jenkins, K. Kornbluth, C. Træholt, "Optimization under uncertainty of a biomass-integrated renewable energy microgrid with energy storage," *Renewable Energy*, vol. 123, pp. 204–217, 2018
- [6] V.S. Tabar, M.A. Jirdehi, R. Hemmati, "Energy management in microgrid based on the multi objective stochastic programming incorporating portable renewable energy resource as demand response option," *Energy*, vol. 118, pp. 827–39, 2017.
- [7] M. Komeili, P. Nazarian, A. Safari, M. Moradlou, "Robust optimal scheduling of CHP-based microgrids in presence of wind and photovoltaic generation units: An IGDT approach," *Sustainable Cities Soc.*, vol. 78, p. 103566, 2022.
- [8] M. Afroozeh, H. R. Abdolmohammadi, M. E. Nazari, "Economic-environmental dispatch of integrated thermal-CHP-heat only system with temperature drop of the heat pipeline using mutant gray wolf optimization algorithm," *Electr. Power Syst. Res.*, vol. 212, p. 108227, 2022.
- [9] M. Alipour, B. Mohammadi-Ivatloo, K. Zare, "Stochastic scheduling of renewable and CHP-based microgrids," *IEEE Trans. Ind. Inf.*, vol. 11, no. 5, pp. 1049–1058, 2019.
- [10] M.H. Imani, M.J. Ghadi, S. Ghavidel, L. Li, "Demand Response Modeling in Microgrid Operation: a Review and Application for Incentive-Based and Time-Based Programs," *Renewable Sustainable Energy Rev.*, vol. 94, pp. 486–499, 2018.
- [11] M.H. Shams, M. Shahabi, M. E. Khodayar, "Stochastic day-ahead scheduling of multiple energy Carrier microgrids with demand response," *Energy*, vol. 155, pp. 326–338, 2018.
- [12] N. Liu, L. He, X. Yu, L. Ma, "Multiparty energy management for grid-connected microgrids with heat-and electricity-coupled demand response," *EEE Trans. Ind. Inf.*, vol. 14, no. 5, pp. 1887–1897, 2018.
- [13] F. Kalavani, B. Mohammadi-Ivatloo, K. Zare, "Optimal stochastic scheduling of cryogenic energy storage with wind power in the presence of a demand response program," *Renewable Energy*, vol. 130, pp. 268–280, 2019.
- [14] M. Sedighzadeh, M. Esmaili, N. Mohammadkhani, "Stochastic multi-objective energy management in residential microgrids with combined cooling, heating, and power units considering battery energy storage systems and plug-in hybrid electric vehicles," *J. Cleaner Prod.*, vol. 195, pp. 301–317, 2018.
- [15] N. Mohammadkhani, M. Sedighzadeh, M. Esmaili, "Energy and emission management of CCHPs with electric and thermal energy storage and electric vehicle," *Therm. Sci. Eng. Prog.*, vol. 8, pp. 494–508, 2018.
- [16] A.S. Langeroudi, M. Sedaghat, S. Pirpoor, R. Fotouhi, M. A. Ghasemi, "Risk-based optimal operation of power, heat and hydrogen-based microgrid considering a plug-in electric vehicle," *Int. J. Hydrogen Energy*, vol. 46, no. 58, pp. 30031–30047, 2021.
- [17] A. Nouri, H. Khodaei, A. Darvishan, S. Sharifian, N. Ghadimi, "Optimal performance of fuel cell-CHP-battery based micro-grid under real-time energy management: an epsilon constraint method and fuzzy satisfying approach," *Energy*, vol. 159, pp. 121–133, 2018.
- [18] S.M. Sadati, A. Rastgou, M. Shafie-khah, S. Bahramara, S. Hosseini-hemati, "Energy management modeling for a community-based electric vehicle parking lots in a power distribution grid," *J. Energy Storage*, vol. 38, p. 102531, 2021.
- [19] F.S. Gazijahani, J. Salehi, "Stochastic multi-objective framework for optimal dynamic planning of interconnected microgrids," *IET Renewable Power Gener.*, vol. 11, no. 14, pp. 1749–1759, 2017.
- [20] F. Kalavani, B. Mohammadi-Ivatloo, K. Zare, "Optimal stochastic scheduling of cryogenic energy storage with wind power in the presence of a demand response program," *Renewable Energy*, vol. 130, pp. 268–280, 2019.
- [21] Y. Li, H. Chen, Y. Ding, "Fundamentals, and applications of cryogen as a thermal energy carrier: A critical assessment," *Int. J. Therm. Sci.*, vol. 49, no. 6, pp. 941–949, 2010.
- [22] H. Khani, M.R. Zadeh, "Real-time optimal dispatch and economic viability of cryogenic energy storage exploiting arbitrage opportunities in an electricity market," *IEEE Trans. Smart Grid*, vol. 6, no. 1, pp. 391–401, 2015.
- [23] Q. Zhang, I.E. Grossmann, C. F. Heuberger, A. Sundaramoorthy, J. M. Pinto, "Air separation with cryogenic energy storage: optimal scheduling considering electric energy and reserve markets," *AIChE J.* vol. 61, no. 5, pp. 1547–1558, 2015.
- [24] J. Salehi, F.S. Gazijahani, A. Safari, "Stochastic simultaneous planning of interruptible loads, renewable generations and capacitors in distribution network," *J. Oper. Autom. Power Eng.*, vol. 10, no. 2, pp. 113–121, 2022.
- [25] N. Taghizadegan, S. Cheshmeh Khavar, A. Abdolahi, F. Arasteh, R. Ghoreyshi, "Dominated GSO algorithm for optimal scheduling of renewable microgrids with penetration of electric vehicles and energy storages considering DRP," *Int. J. Ambient Energy*, vol. 43, no. 1, pp. 6380–6391, 2022.
- [26] J. Olamaei, M.E. Nazari, S. Bahravar, "Economic environmental unit commitment for integrated CCHP-thermal-heat only system with considerations for valve-point effect based on a heuristic optimization algorithm," *Energy*, vol. 159, pp. 737–750, 2018.
- [27] H. Makhdoomi, J. Moshtagh, "Optimal scheduling of electrical storage system and flexible loads to participate

- in energy and flexible ramping product markets,” *J. Oper. Autom.*, vol. 11, no. 3, pp. 203–212, 2023
- [28] N. Daryani, M.T. Hagh, and S. Teimourzadeh, “Adaptive group search optimization algorithm for multi-objective optimal power flow problem,” *Appl. Soft Comput.*, vol. 38, pp. 1012–1024, 2016.
- [29] S. He, Q. H. Wu, and J. Saunders, “Group search optimizer: an optimization algorithm inspired by animal searching behavior,” *EEE Trans. Evol. Comput.*, vol. 13, no. 5, pp. 973–990, 2009.
- [30] F.S. Gazijahani, S. N. Ravadanegh, J. Salehi, “Stochastic multi-objective model for optimal energy exchange optimization of networked microgrids with presence of renewable generation under risk-based strategies,” *ISA Trans.*, vol. 73, pp. 100–111, 2018.
- [31] A. Jani, H. Karimi, S. Jadid, “Hybrid energy management for islanded networked microgrids considering battery energy storage and wasted energy,” *J. Energy Storage*, vol. 40, p. 102700, 2021.
- [32] A. Abdolahi, F.S. Gazijahani, A.A. Alizadeh, N. T. Kalantari, “Chance-constrained CAES and DRP scheduling to maximize wind power harvesting in congested transmission systems considering operational flexibility,” *Sustainable Cities Soc.*, vol. 51, p. 101792, 2019.
- [33] J. Olamaei, M.E. Nazari, S. Bahravar, “Economic environmental unit commitment for integrated CCHP-thermal-heat only system with considerations for valve-point effect based on a heuristic optimization algorithm,” *Energy*, vol. 159, pp. 737–750, 2018.
- [34] M. Alipour, B. Mohammadi-Ivatloo, K. Zare, “Stochastic scheduling of renewable and CHP-based microgrids,” *IEEE Trans. Ind. Inf.*, vol. 11, no. 5, pp. 1049–1058, 2015.
- [35] A. Abdolahi, J. Salehi, F.S. Gazijahani, A. Safari, “Assessing the potential of merchant energy storage to maximize social welfare of renewable-based distribution networks considering risk analysis,” *Electr. Power Syst. Res.*, vol. 188, p. 106522, 2022
- [36] M. Shamshirband, J. Salehi, F.S. Gazijahani, “Decentralized trading of plug-in electric vehicle aggregation agents for optimal energy management of smart renewable penetrated microgrids with the aim of CO2 emission reduction,” *J. Cleaner Prod.*, vol. 200, pp. 622–640, 2018.
- [37] Y. Li, Z. Yang, G. Li, D. Zhao, W. Tian, “Optimal scheduling of an isolated microgrid with battery storage considering load and renewable generation uncertainties,” *EEE Trans. Ind. Electron.*, vol. 66, no. 2, pp. 1565–1575, 2018.
- [38] M. Bornapour, R.A. Hooshmand, M. Parastegari, “An efficient scenario-based stochastic programming method for optimal scheduling of CHP-PEMFC, WT, PV and hydrogen storage units in micro grids,” *Renewable energy*, vol. 130, pp. 1049–1066, 2019.
- [39] X. Zeng, M. S. Nazir, M. Khaksar, K. Nishihara, H. Tao, “A Day-ahead economic scheduling of microgrids equipped with plug-in hybrid electric vehicles using modified shuffled frog leaping algorithm,” *J. Energy Storage*, vol. 33, p. 102021, 2021.
- [40] Y. Li, K. Li, Z. Yang, Y. Yu, R. Xu, M. Yang, “Stochastic optimal scheduling of demand response-enabled microgrids with renewable generations: An analytical-heuristic approach,” *J. Cleaner Prod.*, vol. 30, p. 129840, 2022.
- [41] Y. W. Liu, L.L. Li, M.L. Tseng, M.K. Lim, M. Helmi Ali, “Optimal scheduling of combined cooling, heating, and power microgrid based on a hybrid gray wolf optimizer,” *J. Ind. Prod. Eng.*, vol. 39, no. 4, pp. 277–292, 2022.
- [42] R. Khorram-Nia, B. Bahmani-Firouzi, M. Simab, “Optimal scheduling of reconfigurable microgrids incorporating the PEVs and uncertainty effects,” *IET Renewable Power Gener.*, vol. 16, no. 16, pp. 3531–3543, 2022.
- [43] L. Luo, S.S. Abdulkareem, A. Rezvani, M. R. Miveh, S. Samad, N. Aljojo, M. Pazhoohesh, “Optimal scheduling of a renewable based microgrid considering photovoltaic system and battery energy storage under uncertainty,” *J. Energy Storage*, vol. 28, p. 101306, 2020.